Hydrol. Earth Syst. Sci. Discuss., 11, 12027–12062, 2014
www.hydrol-earth-syst-sci-discuss.net/11/12027/2014/
doi:10.5194/hessd-11-12027-2014

Hydrology and Earth System Sciences
Discussions
Open Access

GRACE storage-streamflow hystereses reveal the dynamics of regional watersheds

E. A. Sproles[1,2,3], **S. G. Leibowitz**[4], **J. T. Reager**[5], **P. J. Wigington Jr.**[4,*], **J. S. Famiglietti**[5], and **S. D. Patil**[6]

[1]Oak Ridge Institute for Science and Technology, c/o National Health and Environmental Effects Research Laboratory, US Environmental Protection Agency, 200 SW 35th Street, Corvallis, OR, 97333, USA
[2]Current address: Centro de Estudios en Zonas Áridas, Universidad de La Serena, Raul Bitran 1305, La Serena, Chile
[3]College of College of Earth, Ocean, and Atmospheric Sciences, Oregon State University, Corvallis, OR, 97331-5503, USA
[4]National Health and Environmental Effects Research Laboratory, US Environmental Protection Agency, 200 SW 35th Street, Corvallis, OR, 97333, USA
[5]Jet Propulsion Laboratory, California Institute of Technology, Pasadena, California, 91109, USA
[6]School of Environment, Natural Resources and Geography, Bangor University, Bangor, LL57 2UW, Wales
[*]retired

Received: 23 September 2014 – Accepted: 10 October 2014 – Published: 30 October 2014

Correspondence to: E. A. Sproles (eric.sproles@gmail.com)

Published by Copernicus Publications on behalf of the European Geosciences Union.

Abstract

We characterize how regional watersheds function as simple, dynamic systems through a series of hysteresis loops. These loops illustrate the temporal relationship between runoff and terrestrial water storage using measurements from NASA's Gravity Recovery and Climate Experiment (GRACE) satellites in three regional-scale watersheds (> 150 000 km^2) of the Columbia River Basin, USA and Canada. The direction of the hystereses for the GRACE signal move in opposite directions from the isolated groundwater hystereses, suggesting that regional scale watersheds require soil water storage to reach a certain threshold before groundwater recharge and peak runoff occur. While the physical processes underlying these hystereses are inherently complex, the vertical integration of terrestrial water in the GRACE signal encapsulates the processes that govern the non-linear function of regional-scale watersheds. We use this process-based understanding to test how GRACE data can be applied prognostically to predict seasonal runoff (mean R^2 of 0.91) and monthly runoff (mean R^2 of 0.77) in all three watersheds. The global nature of GRACE data allows this same methodology to be applied in other regional-scale studies, and could be particularly useful in regions with minimal data and in trans-boundary watersheds.

1 Introduction

At the most fundamental level, watershed processes can be described as the collection, storage, and release of water (Black, 1996; McDonnell et al., 2007). At a more complex level, watersheds typically function as non-linear, dynamic systems governed by their unique climate and geology (Kirchner, 2009). Gaining insights into hydrologic processes and behaviors helps to provide a process-based understanding of watersheds as dynamic environmental systems (Aspinall, 2010), and to identify connections that advance hydrologic science and hydrologic prediction (Wagener et al., 2007). At the local scale, in situ instrumentation can quantify the non-linear relationship between streamflow and water stored in a watershed as snow, soil moisture, groundwater and reservoirs (Appleby, 1970; Brutsaert, 2008; Kirchner, 2009; Sayama et al., 2011). These four primary storage components, along with landscape and topography, govern the fluxes of water through a catchment, and play an important role in the hysteretic nature of storage and runoff dynamics (McGlynn and McDonnell, 2003; McNamara et al., 2011). Knowledge of these processes is fundamental to developing an understanding of a watershed's hydrologic behavior. However, observations over larger regions can be technically challenging and costly, and in situ measurements from small basins do not necessarily represent the complexity inherent to watersheds at more broad scales. This scaling problem limits our capacity to understand and predict regional hydrologic processes, which is often the practical scale of watershed management (Blöschl, 2001; Western et al., 2002; Skøien et al., 2003; Peel and Blöschl, 2011; Thompson et al., 2011).

In the absence of large scale observations, past hydrological studies have typically relied on in situ measurements as a proxy for regional scale hydrological processes. For example, in higher latitude or mountainous regions measurements of snow water storage have provided a simple metric that has been used in water resource planning for decades (Cayan, 1996; United States Army Corps of Engineers, 2001), and are often correlated to streamflow gauged downstream (Dozier, 2011). While informative, this approach can often provide hydrological forecasts that are misleading, because point-based measurements do not fully represent the broad-scale variability of rugged mountain terrain (Dozier, 2011; Nolin, 2012; Webster et al., 2014; Ayala et al., 2014). Similarly, measurements of soil moisture in the upper 2000 mm of the soil rely on point-based data that are often distributed at the regional scale, but do not effectively represent the true variability of soil moisture found at the regional scale (Western et al., 2002; Brocca et al., 2010). A complete understanding of groundwater stores and fluxes (deeper than 2000 mm) at regional scales also remains elusive, despite its increasing importance in water resources management (Wagener et al., 2007; Gleeson et al., 2012; Famiglietti and Rodell, 2013; Barthel, 2014). In addition to contributing to streamflow, groundwater serves as an important water resource for consumptive use (Gleeson et al., 2012). While local-scale methods have been applied with moderate success in the past, current trends in climate and in consumptive water demand suggest that long-term changes in hydrological fluxes will have a major impact at the regional scale (Milly et al., 2008). As a result, the supply and demand of water is also expected to shift, especially at the regional scale (Wagener et al., 2010; Gleick, 2014a).

Hydrologic models can help address the questions of scale and bridge the gap between local scale observations and regional-scale processes by estimating the primary components of water storage (snow, soil moisture, reservoir, and groundwater) across a larger spatial grid. Regional-scale modeling approaches are integrated into water resource management operations for navigation, human consumptive use, irrigation, and hydropower (Payne et al., 2004; Rodell et al., 2004). Models can also be applied diagnostically to test scientific hypotheses and provide a better understanding of the physical processes that govern real world systems, such as the connections between snowmelt, streamflow, and groundwater (Beven, 2007, 2010; Moradkhani and Sorooshian, 2008; Kirchner, 2009; Clark et al., 2011; Capell et al., 2012). Despite their utility, developing and validating a model can be both time consuming and reliant on multiple data inputs, which even in the most well-instrumented basins provides sparse geographic coverage (Bales et al., 2006; Zang et al., 2012). The lack of an integrated measurement of water storage and streamflow has limited regional-scale hydrologic insights to model-based studies (Koster et al., 2010; Mahanama et al., 2011).

Since 2002, broad-scale measurements of changes in the amount of water stored across and through the earth have been available from NASA's Gravity Recovery and Climate Experiment (GRACE) satellites (Tapley et al., 2004). GRACE measures monthly changes in the Earth's gravitational field that are proportional to regional changes in total water storage (Wahr et al., 2006). GRACE satellites provide a monthly record of terrestrial water storage anomalies (TWSA), which represent the changes in the vertical sum of water at the Earth's surface stored in snow, surface, soil and groundwater. Water losses to runoff and evapotranspiration are implicit in the GRACE storage signal, removing the added layer of complexity typically required to model the terrestrial water balance.

GRACE data, coupled with modeled and measured variations of water stored in snow, surface reservoirs and soils, have successfully been decomposed to quantify regional groundwater changes (Rodell et al., 2009; Famiglietti et al., 2011; Voss et al., 2013; Castle et al., 2014) and have contributed to improving water balance calculations (Zaitchik et al., 2008; Li et al., 2012). More recent efforts have quantified the relationship between regional water storage and specific streamflow events (Reager et al., 2014), and have described regional storage-streamflow hysteresis for large basins (Riegger and Tourian, 2014). Although these previous studies have provided new insights into regional watershed hydrology, their analyses are more diagnostic in nature and did not explore the processes behind the observed behavior.

In this paper, we use GRACE observations of terrestrial water storage observations to expand upon a fundamental concept in watershed hydrology – that the temporal relationship between storage and runoff can be used to quantify complex watershed behavior at broad scales, including groundwater recharge amounts and timing, baseflow recession characteristics, and long lead-time streamflow prediction (Brutsaert, 2008; Sayama et al., 2011; Reager et al., 2014; Riegger and Tourian, 2014). The temporal relationship between coincident TWSA and discharge observations at three scales in the Columbia River Basin (CRB) of western North America is investigated using climate and geology as a framing principle to describe the shape of the storage-streamflow hysteresis. We associate regional and temporal differences in the hystereses with varying watershed dynamics. Finally, we compare the prognostic abilities of GRACE observations to individual modeled estimates of snow and soil moisture to predict streamflow at regional scales.

2 Study area

Our study area is the Columbia River Basin (CRB; 41–53° N and 110–122° W). This basin has wet winters, with up to 70 % of annual precipitation falling between November and March, 50–60 % of which occurs as snow (Serreze et al., 1999; Nolin et al., 2012). The spring months (April to June) are also wet, but warmer. Precipitation during the spring combines with snowmelt to swell rivers and potentially exacerbate flooding. Snowmelt also serves as a critical component of the hydrologic cycle recharging aquifers and filling streams later in the year. These contributions bridge the temporal disconnect between wet winters and dry summers when demand is at its peak as farmers, fish, hydropower and municipal users vie for over-allocated water resources (United States Army Corps of Engineers, 2001; Oregon Water Supply and Conservation Initiative, 2008). However, concerns with winter surplus and summer scarcity are not uniform across the CRB, since climate and geology vary greatly. Two of the study watersheds, the Upper Columbia (155 000 km^2) and the Snake River basin (182 000 km^2), represent distinctly different climatic and geologic provinces of the CRB (described and illustrated in Fig. 1). The Upper Columbia is wet and is characterized by steep topography of fractured rock and poor groundwater storage. In contrast, the arid Snake River basin is bowl-shaped with mountains on three sides. The interior of Snake River basin is a broad plain with well-developed soils and high aquifer storage. The Columbia River at The Dalles (614 000 km^2) encompasses the Upper Columbia and the Snake River sub-basins, and its climate and geology are an integration of the two (Fig. 1). A distinct climatic feature of the Columbia River at The Dalles is the western slope of the Cascade Mountains where over 3000 mm of mean annual precipitation at higher elevations sustains a considerable seasonal snowpack. The scale of this study was constrained to watersheds larger than 150 000 km^2, the optimal minimum geographic limit of GRACE data (Yeh et al., 2006; Landerer and Swenson, 2012).

3 Methods and data

We used 108 months of GRACE and streamflow data over nine water years (WY; October–September; 2004–2012). This data comprises positive, neutral, and negative phases of the El Niño–Southern Oscillation and negative and positive phases of the Pacific Decadal Oscillation (Feng et al., 2014; Iizumi et al., 2014). As a result, the data provides years of above- and below-average precipitation, snowpack, and streamflow for the region. The three watersheds were delineated upstream from United States Geological Survey (USGS) stream gages at 1° resolution, which is the resolution of GRACE data (described below). In the CRB, these grid cells represent a dimension of approximately 80 by 120 km. The Upper Columbia consists of the area upstream of the Columbia River at the International Boundary gage (USGS 12399500), just downstream of the confluence of the Columbia and Pend-Oreille Rivers. The Pend-Oreille is a major watershed in the upper portions of the CRB. The Snake River gage at Weiser (USGS 13269000) provides gauged streamflow data above Hell's Canyon Reservoir, the largest impoundment in the Snake River basin. The USGS gage at The Dalles (USGS 14105700) provides the most downstream streamflow data for the CRB. Monthly mean runoff (Q; mm) was calculated for each of the three gages using the USGS streamflow data.

Measurements of TWSA were obtained from the GRACE RL-05 (Swenson and Wahr, 2006; Landerer and Swenson, 2012) data set from NASA's Tellus website (http://grace.jpl.nasa.gov). The errors present in the gridded GRACE data exist primarily as a result of truncation (i.e., a low number of harmonics) in the spherical harmonic solution, and smoothing and systematic noise removal (called "de-striping") that is applied after GRACE level-2 processing to remove spatially correlated noise (called "stripes") (Swenson and Wahr, 2006). This smoothing tends to smear adjacent signals together (within the radius of the filtering function), resulting in smaller signals being lost, and larger signals having a coarser footprint and a loss of spatial information.

Title Page
Abstract | Introduction
Conclusions | References
Tables | Figures
◀| |▶
◀ ▶
Back | Close
Full Screen / Esc
Printer-friendly Version
Interactive Discussion

To restore the GRACE signal lost during processing, the data were scaled using 1° Land-Grid Scale Factors produced by putting a 1° land surface model through identical processing (truncation and filtering) as the GRACE solutions, then measuring the decrease in the signal amplitude at each 1° grid. These procedures are described on the Tellus website and detailed in Landerer and Swenson (2012). Monthly 1° GRACE estimates of TWSA, and the associated 1° leakage and measurement errors, were spatially averaged over each of the three study watersheds following the procedures described in the Tellus website.

GRACE represents monthly storage anomalies relative to an arbitrary record-length mean value, analogous to the amount of water above or below the long-term mean storage of a bucket, and should balance with the equation:

$$\Delta\text{Storage} = \text{TWSA} = \Delta\text{GW} + \Delta\text{SM} + \Delta\text{SWE} + \Delta\text{RES} \qquad (1)$$

where all components are at monthly time steps; GW represents groundwater, SM represents soil moisture (from 0–2000 mm depth), SWE represents snow water equivalent (the equivalent depth of water held in snowpack), and RES represents reservoir storage. The Δ used here represents the anomaly from the study-period mean, rather than a monthly change. To isolate monthly groundwater storage anomalies (ΔGW or GWSA) in the above equation, ΔSM, ΔSWE and ΔRES estimates were subtracted from the monthly TWSA data using methods described in Famiglietti et al. (2011). Monthly SM values over the study basins were obtained from the mean of the North American and Global Land Data Assimilation Systems (NLDAS at 1/8° resolution (Cosgrove et al., 2003) and GLDAS at 1/4° resolution (Rodell et al., 2004), respectively), and were spatially averaged over the three study watersheds. Monthly 1 km resolution SWE values were obtained from the mean of NLDAS and Snow Data Assimilation System (SNODAS; National Operational Hydrologic Remote Sensing Center, 2004) and were spatially averaged over the three watersheds. SNODAS data were used in place of the GLDAS data product, which considerably underestimated SWE in mountainous areas when compared to point-based measurements. Changes in monthly reservoir storage were calculated for the five largest reservoirs in the CRB (see Appendix A). Other smaller reservoirs in the CRB were excluded when it was determined that fluctuations in their levels were below the detection limits of GRACE.

Like all measurements, estimates of TWSA from GRACE contain error. For all of the study basins, the range of error is well below the TWSA signal strength, approximately an order of magnitude below the annual amplitude (200–300 mm) of the TWSA signal in the CRB. The basin-averaged TWSA errors (time invariant) for the three study basins are 37 mm (Upper Columbia), 22 mm (Snake), and 25 mm (The Dalles), and are plotted as bounds on the TWSA time series in Fig. 2a–c. Calculation of the error in individual terms followed standard methodologies (Famiglietti et al., 2011), where error in SM is the mean monthly standard deviation, and standard errors for SWE and RES are 15 % of mean absolute changes. Groundwater anomaly error is the calculated as the sum of basin-averaged errors (added as variance) in the individual terms in the calculation of ΔGW (Eq. 1), including the error in TWSA (Swenson et al., 2006). The basin-averaged error variance for GWSA (time invariant) in the three study basins are 45 mm (Upper Columbia), 26 mm (Snake), and 33 mm (The Dalles), and are plotted as bounds on the GWSA time series in Fig. 2d–f. The individual components (SM, SWE, RES respectively) for each basin are Upper Columbia (24, 6, 0.01 mm), Snake (14, 3, 0.01 mm), and The Dalles (21, 4, 0.01 mm). Note that these error estimates are distributed across an entire regional watershed and do not represent the error at individual monitoring sites.

Based on an approach similar to Reager et al. (2014) and Riegger and Tourian (2014), we plotted the temporal relationship between TWSA and Q to examine hysteresis relationships in all three of the study watersheds for each individual water year and for the monthly mean across all water years. Expanding from the integrated terrestrial component of water storage, we also plotted the relationship between GWSA and Q. We examined the branches of these hysteresis plots to measure basin groundwater recharge amount and timing, storage peak amount and storage peak month. In order to verify groundwater hysteresis, we compared the GRACE-derived GWSA to groundwater depths from well measurements at 33 sites throughout the study region (Fig. 1 and Appendix A). These data were normalized by their standard deviation, and the mean of the 33 wells was calculated. The standard deviation of the GRACE-derived GWSA for The Dalles was normalized to provide a direct comparison of GWSA and in situ measurements.

We further hypothesized that spring TWSA could predict Q later in the year for individual months and after peak SWE accumulation (April–September). To test this prognostic hypothesis we used a two-parameter power function (The MathWorks, 2013) to evaluate the ability of TWSA in March and April to predict cumulative Q from April–September (Q_{season}) and for August (Q_{August}), the low-flow month when demand is near its peak. Additionally, we tested and compared the modeled-values of SWE and soil moisture from NLDAS, GLDAS, and SNODAS to predict Q_{season} and Q_{August} using the same power-function analysis.

4 Results

4.1 Storage-discharge hysteresis plots

The filling and emptying of the study basins at the regional-scale over the course of an individual WY results in a hysteretic relationship between storage and runoff (Fig. 3a). The hysteresis loops begin at the onset of the wet season in October, with TWSA increasing (Figs. 3a and 4a–c) as precipitation is stored as snow and soil moisture. An increase in storage that is not offset by an increase in discharge indicates a predominance of snow inputs and the freezing of soil water. The lower branch of the hysteresis plot (storage increase unmatched by streamflow) can be used to estimate cumulative snow water equivalent and soil moisture in the basin. This is the water that later contributes to streamflow and groundwater recharge in the spring.

The hysteresis shifts direction from February–April (inflection 1, Fig. 3a) when saturated soils and snow melt cause Q to rapidly increase. Each hysteresis loop contains a vertical branch of the curve during which storage is relatively constant, but streamflow increases rapidly. This also represents the groundwater recharge branch of the loop. As snow melts and the ground thaws, runoff is generated, recharge into soils occurs, and basins tend to be at peak storage during this branch. Storage losses and additional precipitation inputs during this period are re-organized internally. A second shift (inflection 2, Fig. 3a) occurs from April–June when peak TWSA begins to decrease, representing spring snowmelt and a switch from precipitation that falls primarily as snow to rain; these combine to contribute to peak Q.

Once peak Q values are reached, the loop shifts direction a third time (inflection 3, Fig. 3a), receding on both axes as contributions from snowmelt diminish while groundwater sustains streams and provides a source for irrigated agriculture. During this period, the relationship between TWSA and discharge is linear, corresponding to baseflow-driven runoff processes in which each monthly change in storage causes a proportional change in the generation of streamflow.

The hysteresis plots of TWSA-Q for an individual water year demonstrate that the timing and quantity of precipitation governs the size of a hysteresis loop for an individual WY (Figs. 3a, 4a–c, and 5). For instance wet years (e.g., 2008) have bigger loops, while dry years (e.g., 2005) are more compressed along both axes. However, the general shape of the loops is distinct for each basin. Plotting multiple WYs provides a family of curves for each basin that helps describe the how climate and geology governs the timing and magnitude of the relationship between TWSA and Q (Figs. 3a–c and 5).

4.2 Individual basin hysteresis plots

Of the three study basins, the Upper Columbia is the most hydrologically responsive, with a mean range of 210 mm for TWSA and 50 mm for Q. The Upper Columbia's steep topography and wet climate fills the limited aquifer quickly, reaching a storage threshold and generating runoff. The steep topography moves snowmelt and rain quickly through the terrestrial system and into the river channel until cresting in June (Figs. 4 and 5), followed by declines in TWSA and Q from June–September.

In contrast to the rapid response of the Upper Columbia, the Snake River receives ~ 60 % less annual precipitation, but has an annual TWSA range that is only 26 % less (160 mm; Figs. 4 and 5). However, the hysteresis loops for the Snake River are collapsed (mean annual range in $Q = 7$ mm). The climate and geology of the Columbia River at The Dalles (Figs. 4 and 5) are an integration of the Upper Columbia and Snake River, seen in the shape of the hysteresis loops (mean ranges TWSA = 180 mm; $Q = 25$ mm). The period from February–June more closely resembles the Snake River basin, with gradual increases in TWSA and sharp increases in Q. The slope of the recession from June–September has the same general shape for The Dalles as the Upper Columbia (Fig. 4a and c), presumably from snowmelt-generated runoff.

4.3 Groundwater-discharge hysteresis plots

The hysteresis loops describing the temporal relationship between GWSA and Q are equally informative, with one dramatic difference – they temporally progress in opposite directions of the hysteresis loops of TWSA and Q (Fig. 3). For all three watersheds, GWSA decreased from October–February/March (Fig. 4d–f), and does not shift towards positive gains until early spring and the initial stages of melt before reaching its maximum in June. The 33 point-specific well data show considerable individual variability throughout a water year, and the mean of the mean of the standard deviations was close to zero for all months (Fig. 6).

4.4 Streamflow forecasting

We next present how TWSA was applied prognostically to predict streamflow. $\text{TWSA}_{\text{March}}$ can predict the total Q from April through September (Q_{season}) in all three basins with an R^2 range of 0.83–0.98 and a mean R^2 ($\overline{R}^2$) of 0.91 (Fig. 7a, Table 1). Applying TWSA for April also provided similar results, but with a lower degree of skill in predicting Q (range = 0.75–0.92, $\overline{R}^2 = 0.86$).

TWSA$_{\text{March}}$ also served as a good indicator of August runoff (Q_{August}, range = 0.68–0.88, $\overline{R}^2 = 0.77$). While this overall mean is high, the range of agreement between basins was not uniform (Fig. 7b). The skill of TWSA$_{\text{March}}$ in the Snake River ($R^2 = 0.68$) was considerably lower than the Columbia River at The Dalles ($R^2 = 0.88$).

Snowpack and soil moisture play a considerable role in the hydrology of the CRB and are commonly used to help predict water demand and availability later in the year (Koster et al., 2010). We compared the predictive capabilities of the modeled snow (SWE) and soil moisture (SM) products to the GRACE TWSA data (Table 1). Compared to SWE, TWSA$_{\text{March}}$ provided a better indicator of seasonal and August runoff in the Upper Columbia and at the Dalles across all nine years (Fig. 6). In the Snake River, SM provided a slightly higher degree of skill than TWSA$_{\text{March}}$ in predicting Q_{season} and Q_{August}. However in the Upper Columbia and The Dalles, SM provided inferior predictive skill for Q_{season} and Q_{August} as compared to TWSA.

5 Discussion

Decades of data collection and monitoring at individual gage sites indicate that watersheds collect, store and release water. Using one integrated measurement from the GRACE satellites our results show these same process at the regional scale in the hysteresis loops of storage (TWSA) and runoff (Q). While hystereic processes have previously been identified in local-scale measurements (McDonnell, 2003; McGlynn and McDonnell, 2003), only recently has streamflow-storage hysteresis been measured at the regional scale (Riegger and Tourian, 2014).

Our work builds on Riegger and Tourian's (2014) results, and employs GRACE data to describe how regional watersheds function as integrated, non-linear systems governed by climate and geology. Climate controls the size of the hysteresis loops by providing a first-order control on hydrologic inputs and the storage of solid water, which in turn governs the ranges of TWSA and Q. However, runoff response to precipitation and snowmelt does not act independently from geology (Jefferson et al., 2008; Tague et al., 2008), which controls how liquid water is stored and routed through a watershed, even at the regional scale. This in turn helps govern the shape of a watershed's hysteresis curve.

For example, basin steep slopes and fractured bedrock geology in the Upper Columbia cause snowmelt and precipitation to run off quickly, and a relatively small amount is retained in the soil. This phenomena is seen in the more open shape of the hysteresis curve in the Upper Columbia – once maximum TWSA is reached in March, it quickly transitions to runoff (Fig. 4a). These data suggest that this is a watershed where snow storage is the primary component of water storage, which is also reflected in the comparison of SWE and SM data (not shown).

In contrast, the arid and groundwater dominated Snake River basin results provide a very different family of hysteresis curves (Figs. 4 and 5) that are compressed vertically (Q) as compared to the Upper Columbia basin, despite showing a similar intra-annual range horizontally (TWSA). Another distinction is that the onset of spring melt runoff in February does not deplete TWSA at the Snake River. Instead, TWSA continues to increase until May, when peak runoff occurs. These data support the conceptual model of a watershed that retains comparatively more winter precipitation in soils and aquifers throughout the spring season, and that drains to sustain flow later in the year.

The greater Columbia River Basin upstream from The Dalles integrates the climatic and geologic characteristics of the Snake River and Upper Columbia as well as other areas within the CRB. The western slope of the Cascades, which is outside of the Upper Columbia, accumulates up to several meters of SWE each winter. The region due east of the Cascades is characterized by a plain underlain by basalt that provides excellent aquifer storage and helps dampen the snowmelt pulse in the spring. The hysteresis loops for the CRB reflect these combined characteristics, where the onset of melt in February produces a pronounced increase in runoff similar to the Upper Columbia. However, as with the Snake River, increases in measured TWSA are found in the CRB through April.

Title Page
Abstract | Introduction
Conclusions | References
Tables | Figures
◀| |▶
◀ ▶
Back | Close
Full Screen / Esc
Printer-friendly Version
Interactive Discussion

We applied these climatic and geologic insights to develop and test the hypothesis that spring TWSA could predict Q later in the year, based on two observations: First, the shapes of the hysteresis curves for each basin are similar (Figs. 4a–c and 5), but vary by magnitude of annual TWSA. Second, peak TWSA occurs before the peak runoff. We show that the integrated GRACE signal is a good baseline measurement in predicting seasonal streamflow across a range of water years with regards to precipitation and streamflow. In essence, our data suggest that the water stored across and through the Columbia River Basin in March describes the water available for the remainder of the water year. In the CRB and in the northwestern United States, snowpack is commonly used as a metric for predicting spring runoff. Despite its importance to the hydrologic cycle of the region, measurements of $\text{TWSA}_{\text{March}}$ from GRACE provide a better prediction of seasonal and August runoff than model-derived estimates of snowpack. GRACE $\text{TWSA}_{\text{March}}$ also provided a better prediction for runoff than soil moisture, except for the Snake River basin. There March soil moisture provided a better indicator of runoff for the rest of the year, although $\text{TWSA}_{\text{March}}$ had a similar accuracy (Table 1). Despite a relatively short data record, the years of our study represent a wide-range of conditions with regards to climate and streamflow, which is captured in our models and is shown in the box plots to the right of Fig. 7a and b.

Although these results are promising with regards to using GRACE as a predictive tool for water resources, Fig. 7a and b suggest that Q is insensitive to $\text{TWSA}_{\text{March}}$ values below 100 mm. We recognize that all three of these regional watersheds are managed through a complex series of dams and reservoirs that create an altered runoff signal. Water resources managers use point-specific and model-based estimates of water storage in the region to optimize their operations. Additionally, in the fertile plains of the Snake River and lower CRB, broad-scale agriculture relies on both ground- and surface water for irrigation. Water withdrawals would be implicit in the TWSA signal and reduce Q. Subsequent, more detailed analysis would help quantify these effects. However the compilation of a complete irrigation dataset lies outside the scope of this study. We also acknowledge the length of record for this study would ideally be longer.

Regardless of the length of record or anthropogenic influence, climate and geology still provide the first-order controls on water storage that are found in the hysteresis loops. GRACE encapsulates these hydrologic processes through measurements of TWSA. The hysteresis loops expand and contract accordingly during wet and dry years, as the intra-annual relationship between TWSA and Q represents the fluxes of water into and out of the watershed. Despite intra-annual differences, each of the subregional watersheds can be described by a family of hysteresis curves. The predicative capability using TWSA, the vertical sum of water, as compared to snowpack and soil moisture further highlights the integrated nature of water storage in regional hydrology. These integrated measurements of TWSA provide simple, but informative predictions of seasonal and monthly runoff.

GRACE-derived calculations of GWSA also provide insights into the hydrological processes governing groundwater recharge and depletion, as evidenced in the GWSA hysteresis loops. The GWSA-Q curves show an out-of-phase relationship between precipitation and groundwater recharge from the start of the wet season in October until February or March. This suggests that groundwater helps sustain stream flow during the wet fall and winter and that pore space in soils and geologic materials must fill to a certain threshold before groundwater begins to recharge and runoff is generated. The relationship between the TWSA and GWSA curves from October–March identifies how the onset of snowmelt also marks the beginning of groundwater recharge, and suggests that snowmelt inputs to groundwater are considerable. In the CRB this is critical as current climate trends are projected to reduce snowpack accumulation and exacerbate melt in the region (Wu et al., 2012; Rupp et al., 2013; Sproles et al., 2013). Additionally, our analysis identifies summer as the time of peak groundwater storage in all three regional watersheds. This peak corresponds to the timing of groundwater pump tests that are commonly conducted in June, and are used to develop groundwater withdrawal regulations (Jarvis, 2011, 2014). Our data suggest that groundwater pump tests should not be limited to an individual month, and should also include periods of reduced storage particularly during the winter months. The inclusion of multiple pump tests throughout the year could be particularly relevant as the population and water demand is projected to increase in the region.

The point-specific well data (Fig. 6) is ambiguous and show considerable variability with no consistent pattern regarding the timing of recharge and peak groundwater levels (light grey lines in Fig. 6). Rather than excluding these results or selecting individual wells that match GRACE data we include the results from all 33 wells to help demonstrate the variability that exists from well to well, and how site characteristics (i.e., usage, depth, location) might not represent regional groundwater characteristics (Jarvis, 2011, 2014). An in-depth study that couples GWSA and well data would potentially help explain the ambiguity, but lie outside the scope of this study.

GRACE is somewhat of a blunt instrument with regards to temporal (monthly) and spatial (1°) resolution. However, this emerging technology provides a new dimension to regional watershed analysis by providing an integrated measurement of water stored across and through the Earth. These measurements continue to prove their value in retrospective analysis of regional hydrology (Rodell et al., 2009; Castle et al., 2014). However, the hysteresis loops presented here and in Riegger and Tourian (2014) demonstrate the ability of GRACE data to help develop a process-based understanding of how regional watersheds function as simple, dynamic systems. As the temporal record of GRACE continues to develop, its value as both a diagnostic and predictive tool will continue to grow. In the mean time, these data have value in augmenting existing management strategies.

Perhaps one of the most important facets of GRACE data is that it does not distinguish political boundaries, and it is not linked to a specific in situ monitoring agency with limited data access, and has the capacity to bridge sparse and inconsistent on-the-ground hydrologic monitoring networks that exist in many regions of the world. Previous GRACE-based analysis has shown its value in highlighting negative trends in terrestrial water storage in trans-boundary watersheds (Voss et al., 2013; Castle et al., 2014), and resulting regional conflict exacerbated by water shortages (Gleick, 2014b).

GRACE provides an objective measurement of a region's water resources that can provide valuable insights into potential shortages or surpluses of water resources.

6 Conclusions

We have shown how GRACE-based measurements of TWSA distill the complexity of regional hydrology into a simple, dynamic system. TWSA and derived estimates of GWSA reveal hysteretic behavior for regional watersheds, which is more commonly associated with hydrologic measurements at local scales. While the magnitude of the hysteresis curves varies across years, they retain the same general shape that is unique to each watershed. We demonstrated the utility of these hysteresis curves by showing how TWSA during March can be used to predict Q during the drier summer months. Because GRACE-TWSA can augment prediction, managers could start to interpret each year's hysteresis curve for the upcoming spring and summer, providing greater clarity and validation for model-based forecasts presently used by water resource managers.

Although this study focused on the CRB, which has a rich data record, GRACE data are available at a global scale and could be readily applied in areas with a paucity of data to understand how watersheds function and to improve streamflow forecasting capabilities. GRACE does not discern political boundaries and provides an integrated approach to understanding international watersheds (Voss et al., 2013). This resource could serve as a valuable tool for managers in forecasting surplus and scarcity, and in developing strategies that include changes in supply and demand due to human consumptive needs and current climate trends (Wagener et al., 2010; Gleick, 2014a).

Author contributions. E. A. Sproles, S. G. Leibowitz, and P. J. Wigington Jr. developed the hysteresis concept based upon background research by J. T. Reager and J. S. Famiglietti. The data analysis was led by E. A. Sproles, but represents a combined effort from all of the authors. J. T. Reager provided expertise in the GRACE data product, groundwater, and error analysis. E. A. Sproles prepared the manuscript with contributions from all co-authors.

Acknowledgements. The authors would like to thank Matthew Rodell and Felix Landerer for their expertise in understanding GRACE data during the initial stages of the research. GRACE terrestrial data were processed by Sean Swenson, supported by the NASA MEaSUREs Program, and are available at http://grace.jpl.nasa.gov. The GLDAS and NLDAS data used in this study were acquired as part of the mission of NASA's Earth Science Division and archived and distributed by the Goddard Earth Sciences Data and Information Services Center. Additionally, Tim Kerr provided objective feedback and comments on the research findings. The information in this document has been funded entirely by the US Environmental Protection Agency, in part by an appointment to the Internship/Research Participation Program at the Office of Research and Development, US Environmental Protection Agency, administered by the Oak Ridge Institute for Science and Education through an interagency agreement between the US Department of Energy and EPA. This manuscript has been subjected to Agency review and has been approved for publication. Mention of trade names or commercial products does not constitute endorsement or recommendation for use.

References

Appleby, F. V.: Recession and the baseflow problem, Water Resour. Res., 6, 1398–1403, doi:10.1029/WR006i005p01398, 1970.

Aspinall, R.: A century of physical geography research in the Annals, Ann. Assoc. Am. Geogr., 100, 1049–1059, 2010.

Ayala, A., McPhee, J., and Vargas, X.: Altitudinal gradients, midwinter melt, and wind effects on snow accumulation in semiarid midlatitude Andes under La Niña conditions, Water Resour. Res., 50, 3589–3594, doi:10.1002/2013WR014960, 2014.

Bales, R. C., Molotch, N. P., Painter, T. H., Dettinger, M. D., Rice, R., and Dozier, J.: Mountain hydrology of the western United States, Water Resour. Res., 42, W08432, doi:10.1029/2005wr004387, 2006.

Barthel, R.: A call for more fundamental science in regional hydrogeology, Hydrogeol. J., 22, 507–510, 2014.

Beven, K. J.: Towards integrated environmental models of everywhere: uncertainty, data and modelling as a learning process, Hydrol. Earth Syst. Sci., 11, 460–467, doi:10.5194/hess-11-460-2007, 2007.

Beven, K. J.: Preferential flows and travel time distributions: defining adequate hypothesis tests for hydrological process models, Hydrol. Process., 24, 1537–1547, 2010.
Black, P. E.: Watershed Hydrology, CRC Press, Boca Raton, FL, 1996.
Blöschl, G.: Scaling in hydrology, Hydrol. Process., 15, 709–711, 2001.
Brocca, L., Melone, F., Moramarco, T., and Morbidelli, R.: Spatial–temporal variability of soil moisture and its estimation across scales, Water Resour. Res., 50, 3589–3594, doi:10.1002/2013WR014960, 2010.
Brutsaert, W.: Long-term groundwater storage trends estimated from streamflow records: climatic perspective, Water Resour. Res., 44, W02409, doi:10.1029/2007WR006518, 2008.
Capell, R., Tetzlaff, D., Hartley, A. J., and Soulsby, C.: Linking metrics of hydrological function and transit times to landscape controls in a heterogeneous mesoscale catchment, Hydrol. Process., 26, 405–420, 2012.
Castle, S. L., Thomas, B. F., Reager, J. T., Rodell, M., Swenson, S. C., and Famiglietti, J. S.: Groundwater depletion during drought threatens future water security of the Colorado River Basin, Geophys. Res. Lett., 41, 5904–5911, doi:10.1002/2014GL061055, 2014.
Cayan, D. R.: Interannual climate variability and snowpack in the western United States, J. Climate, 9, 928–948, doi:10.1175/1520-0442(1996)009<0928:ICVASI>2.0.CO;2, 1996.
Clark, M. P., Kavetski, D., and Fenicia, F.: Pursuing the method of multiple working hypotheses for hydrological modeling, Water Resour. Res., 47, W09301, doi:10.1029/2010WR009827, 2011.
Cosgrove, B. A., Lohmann, D., Mitchell, K. E., Houser, P. R., Wood, E. F., Schaake, J. C., Robock, A., Marshall, C., Sheffield, J., and Duan, Q.: Real-time and retrospective forcing in the North American Land Data Assimilation System (NLDAS) project, J. Geophys. Res., 108, 8842, doi:10.1029/2002JD003118, 2003.
Dozier, J.: Mountain hydrology, snow color, and the fourth paradigm, EOS T. Am. Geophys. Un., 92, 373, doi:10.1029/2011EO430001, 2011.
Famiglietti, J. S. and Rodell, M.: Water in the balance, Science, 340, 1300–1301, 2013.
Famiglietti, J. S., Lo, M., Ho, S. L., Bethune, J., Anderson, K. J., Syed, T. H., Swenson, S. C., de Linage, C. R., and Rodell, M.: Satellites measure recent rates of groundwater depletion in California's Central Valley, Geophys. Res. Lett., 38, L03403, doi:10.1029/2010gl046442, 2011.
Feng, J., Wang, L., and Chen, W.: How does the East Asian summer monsoon behave in the decaying phase of El Niño during different PDO phases?, J. Climate, 27, 2682–2698, 2014.

Gleeson, T., Wada, Y., Bierkens, M. F. P., and van Beek, L. P. H.: Water balance of global aquifers revealed by groundwater footprint, Nature, 488, 197–200, 2012.

Gleick, P. H.: Water, drought, climate change, and conflict in Syria, Weather Clim. Soc., 6, 331–340, 2014a.

Gleick, P. H.: The World's Water Volume 8: The Biennial Report on Freshwater Resources, Island Press, Washington, D.C., 2014b.

Iizumi, T., Luo, J.-J., Challinor, A. J., Sakurai, G., Yokozawa, M., Sakuma, H., Brown, M. E., and Yamagata, T.: Impacts of El Niño Southern Oscillation on the global yields of major crops, Nat. Commun., 5, 3712, doi:10.1038/ncomms4712, 2014.

Jarvis, W. T.: Unitization: a lesson in collective action from the oil industry for aquifer governance, Water Int., 36, 619–630, 2011.

Jarvis, W. T.: Contesting Hidden Waters: Conflict Resolution for Groundwater and Aquifers, Routledge, Abingon, Oxnon, UK, 2014.

Jefferson, A., Nolin, A., Lewis, S., and Tague, C.: Hydrogeologic controls on streamflow sensitivity to climate variation, Hydrol. Process., 22, 4371–4385, doi:10.1002/hyp.7041, 2008.

Kirchner, J. W.: Catchments as simple dynamical systems: catchment characterization, rainfall–runoff modeling, and doing hydrology backward, Water Resour. Res., 45, W02429, doi:10.1029/2008WR006912, 2009.

Koster, R. D., Mahanama, S. P. P., Livneh, B., Lettenmaier, D. P., and Reichle, R. H.: Skill in streamflow forecasts derived from large-scale estimates of soil moisture and snow, Nat. Geosci., 3, 613–616, 2010.

Landerer, F. W. and Swenson, S. C.: Accuracy of scaled GRACE terrestrial water storage estimates, Water Resour. Res., 48, W04531, doi:10.1029/2011wr011453, 2012.

Li, B., Rodell, M., Zaitchik, B. F., Reichle, R. H., Koster, R. D., and van Dam, T. M.: Assimilation of GRACE terrestrial water storage into a land surface model: evaluation and potential value for drought monitoring in western and central Europe, J. Hydrol., 446, 103–115, 2012.

Mahanama, S., Livneh, B., Koster, R., Lettenmaier, D., and Reichle, R.: Soil Moisture, Snow, and Seasonal Streamflow Forecasts in the United States, J. Hydrometeorol., 13, 189–203, doi:10.1175/JHM-D-11-046.1, 2011.

McDonnell, J. J.: Where does water go when it rains? Moving beyond the variable source area concept of rainfall–runoff response, Hydrol. Process., 17, 1869–1875, doi:10.1002/hyp.5132, 2003.

McDonnell, J. J., Sivapalan, M., Vache, K., Dunn, S., Grant, G., Haggerty, R., Hinz, C., Hooper, R., Kirchner, J., Roderick, M. L., Selker, J., and Weiler, M.: Moving beyond heterogeneity and process complexity: a new vision for watershed hydrology, Water Resour. Res., 43, W07301, doi:10.1029/2006wr005467, 2007.

McGlynn, B. L. and McDonnell, J. J.: Quantifying the relative contributions of riparian and hillslope zones to catchment runoff, Water Resour. Res., 39, 1310, doi:10.1029/2003WR002091, 2003.

McNamara, J. P., Tetzlaff, D., Bishop, K., Soulsby, C., Seyfried, M., Peters, N. E., Aulenbach, B. T., and Hooper, R.: Storage as a metric of catchment comparison, Hydrol. Process., 25, 3364–3371, doi:10.1002/hyp.8113, 2011.

Milly, P. C. D., Betancourt, J., Falkenmark, M., Hirsch, R. M., Kundzewicz, Z. W., Lettenmaier, D. P., and Stouffer, R. J.: Stationarity is dead: whither water management?, Science, 319, 573–574, doi:10.1126/science.1151915, 2008.

Moradkhani, H. and Sorooshian, S.: General review of rainfall–runoff modeling: model calibration, data assimilation, and uncertainty analysis, Water Trans., 63, 1–24, 2008.

National Operational Hydrologic Remote Sensing Center: Snow Data Assimilation System (SNODAS) Data Products at NSIDC, (2003–2012), National Snow and Ice Data Center, Boulder, CO, USA, 2004.

Nolin, A. W.: Perspectives on climate change, mountain hydrology, and water resources in the Oregon Cascades, USA, Mt. Res. Dev., 32, S35–S46, doi:10.1659/mrd-journal-d-11-00038.s1, 2012.

Nolin, A. W., Sproles, E. A., and Brown, A.: Climate change impacts on snow and water resources in the Columbia, Willamette, and McKenzie River Basins, USA: a nested watershed study, in: Transboundary River Governance in the Face of Uncertainty: the Columbia River Treaty, edited by: Cosens, B., Oregon State University Press, Corvallis, OR, 2012.

Oregon Water Supply and Conservation Initiative: Southern Willamette Valley Municipal Water Providers Final Report, Salem, Oregon, 2008.

Payne, J. T., Wood, A. W., Hamlet, A. F., Palmer, R. N., and Lettenmaier, D. P.: Mitigating the effects of climate change on the water resources of the Columbia River Basin, Climatic Change, 62, 233–256, 2004.

Peel, M. C. and Blöschl, G.: Hydrological modelling in a changing world, Prog. Phys. Geogr., 35, 249–261, 2011.

Reager, J. T., Thomas, B. F., and Famiglietti, J. S.: River basin flood potential inferred using GRACE gravity observations at several months lead time, Nat. Geosci., 7, 588–592, doi:10.1038/ngeo2203, 2014.

Riegger, J. and Tourian, M. J.: Characterization of runoff–storage relationships by satellite gravimetry and remote sensing, Water Resour. Res., 50, 3444–3466, 2014.

Rodell, M., Houser, P. R., Jambor, U., Gottschalck, J., Mitchell, K., Meng, C. J., Arsenault, K., Cosgrove, B., Radakovich, J., Bosilovich, M., Entin, J. K., Walker, J. P., Lohmann, D., and Toll, D.: The global land data assimilation system, B. Am. Meteorol. Soc., 85, 381–394, doi:10.1175/bams-85-3-381, 2004.

Rodell, M., Velicogna, I., and Famiglietti, J. S.: Satellite-based estimates of groundwater depletion in India, Nature, 460, 999–1002, 2009.

Rupp, D. E., Abatzoglou, J. T., Hegewisch, K. C., and Mote, P. W.: Evaluation of CMIP5 20th century climate simulations for the Pacific Northwest USA, J. Geophys. Res. Atmos., 118, 10884–10906, doi:10.1002/jgrd.50843, 2013.

Sayama, T., McDonnell, J. J., Dhakal, A., and Sullivan, K.: How much water can a watershed store?, Hydrol. Process., 25, 3899–3908, doi:10.1002/hyp.8288, 2011.

Serreze, M. C., Clark, M. P., Armstrong, R. L., McGinnis, D. A., and Pulwarty, R. S.: Characteristics of the western United States snowpack from snowpack telemetry (SNOTEL) data, Water Resour. Res., 35, 2145–2160, doi:10.1029/1999wr900090, 1999.

Skøien, J. O., Blöschl, G., and Western, A. W.: Characteristic space scales and timescales in hydrology, Water Resour. Res., 39, 1304, doi:10.1029/2002WR001736, 2003.

Sproles, E. A., Nolin, A. W., Rittger, K., and Painter, T. H.: Climate change impacts on maritime mountain snowpack in the Oregon Cascades, Hydrol. Earth Syst. Sci., 17, 2581–2597, doi:10.5194/hess-17-2581-2013, 2013.

Swenson, S. and Wahr, J.: Post-processing removal of correlated errors in GRACE data, Geophys. Res. Lett., 33, L08402, doi:10.1029/2005gl025285, 2006.

Swenson, S., Yeh, P. J. F., Wahr, J., and Famiglietti, J.: A comparison of terrestrial water storage variations from GRACE with in situ measurements from Illinois, Geophys. Res. Lett., 33, L16401, doi:10.1029/2006gl026962, 2006.

Tague, C., Grant, G., Farrell, M., Choate, J., and Jefferson, A.: Deep groundwater mediates streamflow response to climate warming in the Oregon Cascades, Climate Change, 86, 189–210, 2008.

Tapley, B. D., Bettadpur, S., Ries, J. C., Thompson, P. F., and Watkins, M. M.: GRACE measurements of mass variability in the Earth system, Science, 305, 503–505, 2004.

The MathWorks: MATLAB and Statistics Toolbox Release 2013a, Natick, Massachusetts, 2013.

Thompson, S. E., Harman, C. J., Schumer, R., Wilson, J. S., Basu, N. B., Brooks, P. D., Donner, S. D., Hassan, M. A., Packman, A. I., and Rao, P. S. C.: Patterns, puzzles and people: implementing hydrologic synthesis, Hydrol. Process., 25, 3256–3266, 2011.

United States Army Corps of Engineers: Comprehensive Water Supply Study – An Examination of Current Water Supply Issues, edited by: Hillyer, T. M., Alexandria, Virginia, 2001.

Voss, K. A., Famiglietti, J. S., Lo, M., Linage, C., Rodell, M., and Swenson, S. C.: Groundwater depletion in the Middle East from GRACE with implications for transboundary water management in the Tigris–Euphrates–Western Iran region, Water Resour. Res., 49, 904–914, doi:10.1002/wrcr.20078, 2013.

Wagener, T., Sivapalan, M., Troch, P., and Woods, R.: Catchment classification and hydrologic similarity, Geogr. Compass, 1, 901–931, doi:10.1111/j.1749-8198.2007.00039.x, 2007.

Wagener, T., Sivapalan, M., Troch, P. A., McGlynn, B. L., Harman, C. J., Gupta, H. V, Kumar, P., Rao, P. S. C., Basu, N. B., and Wilson, J. S.: The future of hydrology: an evolving science for a changing world, Water Resour. Res., 46, W05301, doi:10.1029/2009WR008906, 2010.

Wahr, J., Swenson, S., and Velicogna, I.: Accuracy of GRACE mass estimates, Geophys. Res. Lett., 33, L06401, doi:10.1029/2005gl025305, 2006.

Webster, C. S., Kingston, D. G., and Kerr, T.: Inter-annual variation in the topographic controls on catchment-scale snow distribution in a maritime alpine catchment, New Zealand, Hydrol. Process., doi:10.1002/hyp.10224, in press, 2014.

Western, A. W., Grayson, R. B., and Blöschl, G.: Scaling of soil moisture: a hydrologic perspective, Annu. Rev. Earth Pl. Sc., 30, 149–180, 2002.

Wu, H., Kimball, J. S., Elsner, M. M., Mantua, N., Adler, R. F., and Stanford, J.: Projected climate change impacts on the hydrology and temperature of Pacific Northwest rivers, Water Resour. Res., 48, W11530, doi:10.1029/2012wr012082, 2012.

Yeh, P. J. F., Swenson, S. C., Famiglietti, J. S., and Rodell, M.: Remote sensing of groundwater storage changes in Illinois using the Gravity Recovery and Climate Experiment (GRACE), Water Resour. Res., 42, W12203, doi:10.1029/2006wr005374, 2006.

Zaitchik, B. F., Rodell, M., and Reichle, R. H.: Assimilation of GRACE terrestrial water storage data into a land surface model: results for the Mississippi River Basin, J. Hydrometeorol., 9, 535–548, doi:10.1175/2007JHM951.1, 2008.

Zang, C. F., Liu, J., van der Velde, M., and Kraxner, F.: Assessment of spatial and temporal patterns of green and blue water flows under natural conditions in inland river basins in Northwest China, Hydrol. Earth Syst. Sci., 16, 2859–2870, doi:10.5194/hess-16-2859-2012, 2012.

Table 1. Results from all three study basins using GRACE TWSA data to predict seasonal (Q_{season}) and August (Q_{August}) streamflow as compared to using model derived snow (SWE) and soil moisture (SM) products. Average values for the three basins are also provided. RMSE values are in mm.

	Q_{season}				Q_{Aug}			
Upper Columbia Basin								
	TWSA_{Mar}	TWSA_{Apr}	SWE_{Mar}	SM_{Mar}	TWSA_{Mar}	TWSA_{Apr}	SWE_{Mar}	SM_{Mar}
R^2	0.93	0.92	0.82	0.03	0.76	0.73	0.56	0.09
RMSE	22.18	23.18	36.19	82.90	6.60	6.90	8.92	12.79
Snake River Basin								
	TWSA_{Mar}	TWSA_{Apr}	SWE_{Mar}	SM_{Mar}	TWSA_{Mar}	TWSA_{Apr}	SWE_{Mar}	SM_{Mar}
R^2	0.83	0.75	0.34	0.93	0.68	0.52	0.62	0.76
RMSE	8.76	10.55	17.23	5.80	0.43	0.52	0.47	0.37
The Dalles								
	TWSA_{Mar}	TWSA_{Apr}	SWE_{Mar}	SM_{Mar}	TWSA_{Mar}	TWSA_{Apr}	SWE_{Mar}	SM_{Mar}
R^2	0.98	0.91	0.67	0.00	0.88	0.91	0.46	0.02
RMSE	6.22	13.00	24.60	42.67	1.55	1.30	3.30	4.40
Average								
	TWSA_{Mar}	TWSA_{Apr}	SWE_{Mar}	SM_{Mar}	TWSA_{Mar}	TWSA_{Apr}	SWE_{Mar}	SM_{Mar}
R^2	0.91	0.86	0.61	0.32	0.77	0.72	0.54	0.29
RMSE	12	16	26	44	3	3	4	6

Table A1. The reservoirs used in the GRACE analysis.

Reservoir Name	Operating agency	Normal operating capacity (m^3)
Grand Coulee	US Department of Interior	1.16×10^{10}
Libby	US Army Corps of Engineers	7.17×10^{9}
Hungry Horse	US Department of Interior	4.28×10^{9}
Dworsha	US Army Corps of Engineers	4.26×10^{9}
American Falls	US Department of Interior	2.10×10^{9}

Table A2. The groundwater wells used in the analysis that compares GRACE-derived groundwater with location-specifc wells. USGS is the United States Geological Survey and IDWR is the Idaho Department of Water Resources.

Well number	Operating agency
434400121275801	USGS
442242121405501	USGS
452855119064701	USGS
453239119031501	USGS
453845121191401	USGS
453937121215801	USGS
453944121211301	USGS
454013121225901	USGS
454027121212501	USGS
454040121222901	USGS
454047121203701	USGS
454100119164801	USGS
454416119212801	USGS
455418118333001	USGS
461518114090802	USGS
463750114033001	USGS
465520114074001	USGS
470049113035401	USGS
470946114013201	USGS
473442118162201	USGS
474011117072901	USGS
474251114385201	USGS
475439116503401	USGS
480519114091001	USGS
480621115244901	USGS
02S20E-01ACC2	IDWR
07S06E-29BBA1	IDWR
08S06E-03BDC1	IDWR
07S06E-34BCA1	IDWR
09S14E-03BAA1	IDWR
08S14E-16CBB1	IDWR
05S31E-27ABA1	IDWR
07N38E-23DBA1	IDWR

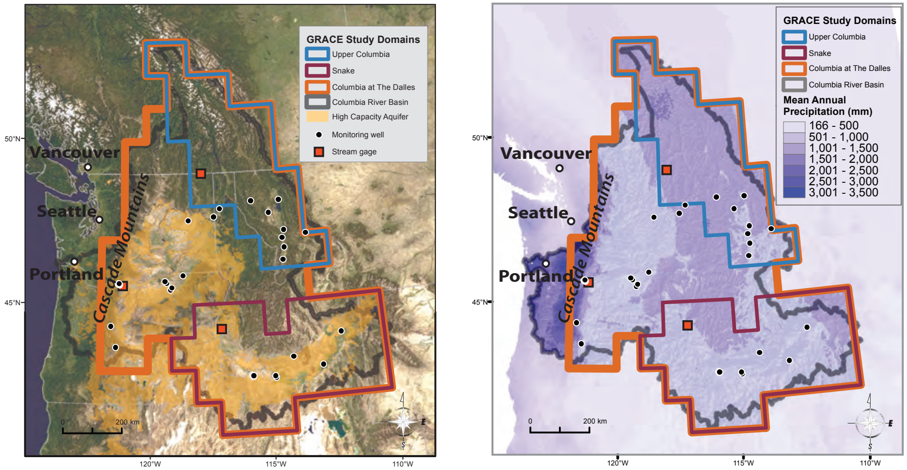

Watershed	Physical Characteristics	Climate
Upper Columbia (155,000 km²)	- Steep topography - Low aquifer storage - Responsive runoff	Wet maritime conditions with 900 mm of annual precipitation, and substantial snowpack accumulation
Snake River (182,000 km²)	- Low relief topography - High aquifer storage - Muted runoff	Dry continental climate with 350 mm of annual precipitation, falling primarily at upper elevations as snow
The Dalles (614,000 km²)	- Includes the Upper Columbia and Snake River - Topography is a blend of the Upper Columbia and Snake River - High storage capacity - Large system that floods	Mix of dry continental climate plains and wet uplands. Mean annual precipitation is 625 mm, with considerable snowpack accumulation in the mountains

Figure 1. Context map and descriptions of the three study watersheds.

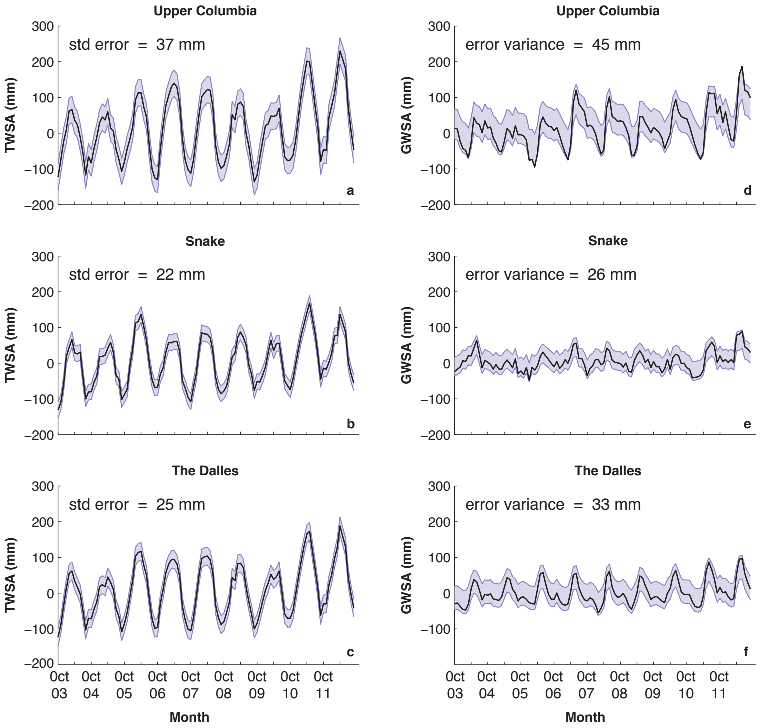

Figure 2. Monthly storage anomalies for TWSA **(a–c)** and GWSA **(d–f)** for the three watersheds. Standard errors **(a)** and error variance **(b)** for each watershed are represented by the blue shading.

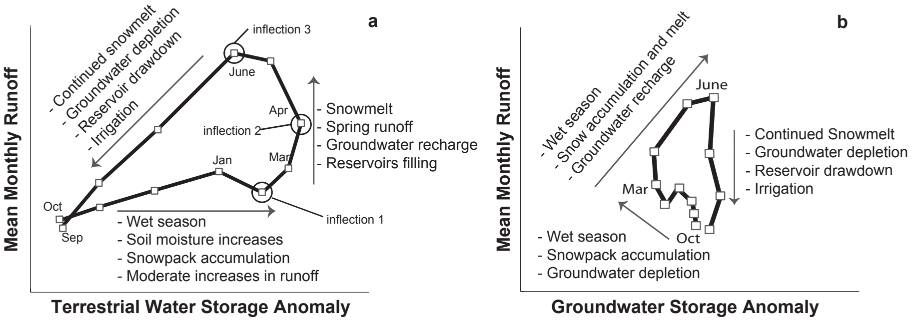

Figure 3. Annotated hysteresis curves of terrestrial water storage anomalies **(a)** and groundwater storage anomalies **(b)** based upon the nine-year mean for the Columbia River at The Dalles. These curves describe the fluxes of water moving through the watershed.

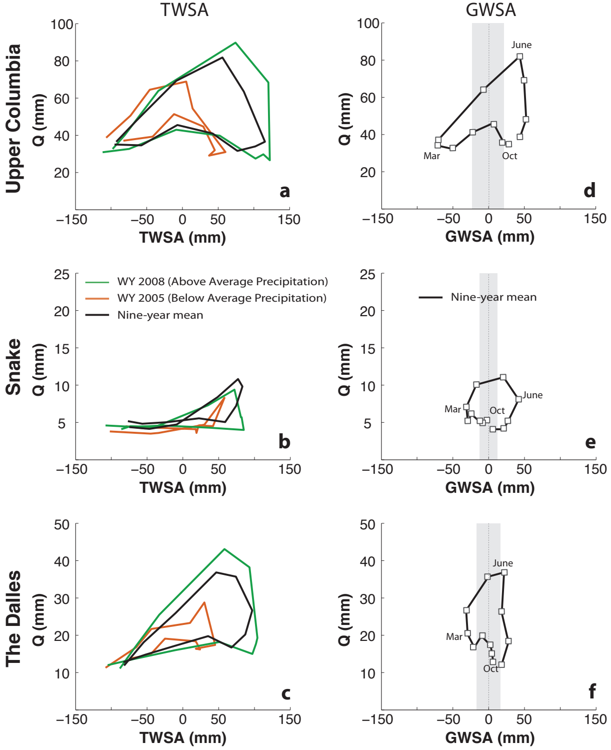

Figure 4. Individual hysteresis curves for the three study watersheds for terrestrial water storage anomaly (TWSA; **a–c**) and groundwater storage anomaly (GWSA; **d–f**). The grey areas in the GWSA plots provide a visual reference of the error variance for each watershed. The low topography and high storage capacity of the Snake aquifer provides a consistent groundwater signal, as compared to the limited aquifer of the Upper Columbia, which fills and drains quickly. Note the different scales on the *y* axes.

Title Page
Abstract Introduction
Conclusions References
Tables Figures
◀I ▶I
◀ ▶
Back Close
Full Screen / Esc
Printer-friendly Version
Interactive Discussion

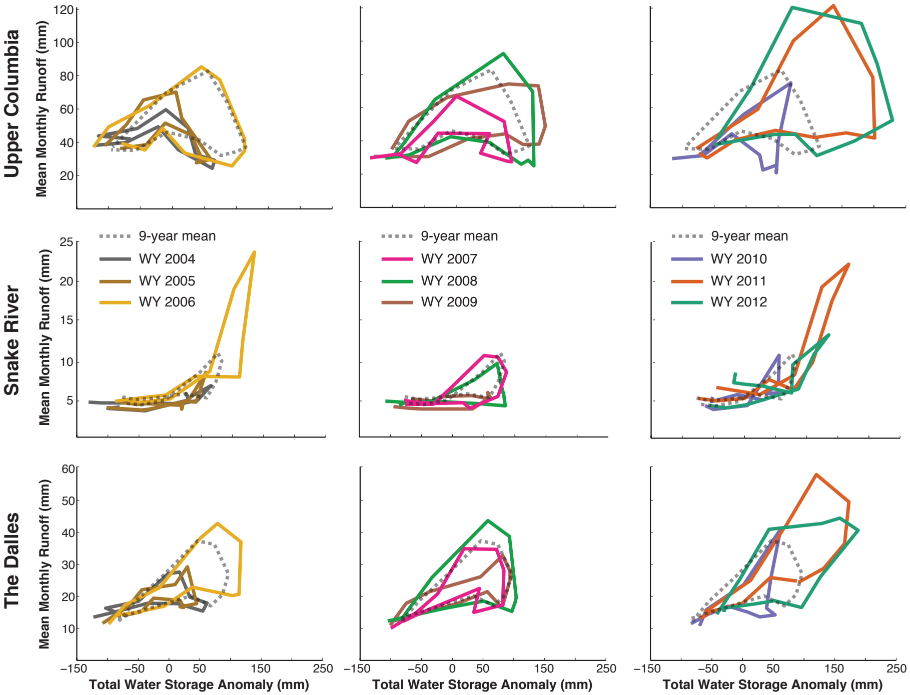

Figure 5. Plots of the hysteresis curves for TWSA in each of the three study watersheds across all nine water years. For visual clarity, each plot contains three water years and the nine-year mean. Note the different scales on the y axes for each basin.

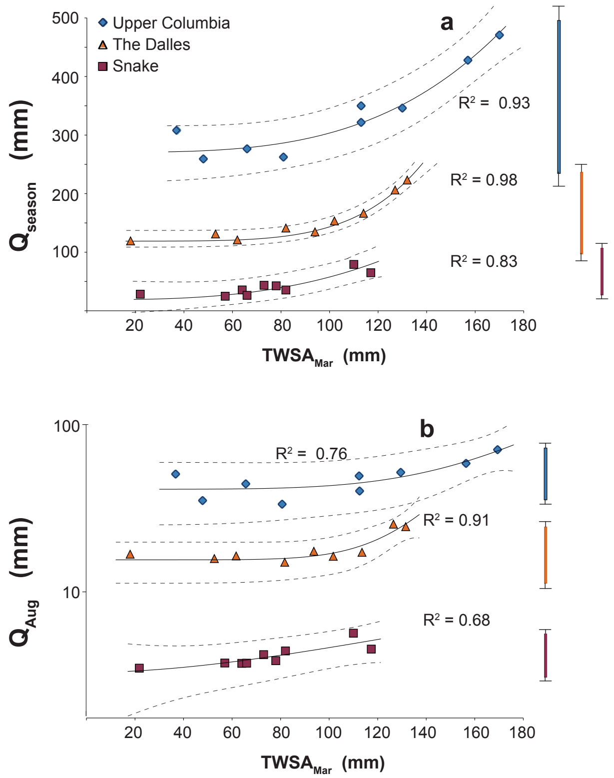

Figure 6. Measurements of terrestrial water storage anomalies in March ($TWSA_{March}$) effectively predict the cumulative runoff for April–September (Q_{season}; **a**), and describe how these three regional watersheds function as simple non-linear systems. $TWSA_{March}$ also predicts mean runoff for August (Q_{August}; **b**), one of the driest months of the year when demand for water is at its peak. The hashed lines represent the 95 % confidence intervals. The box plots to the right of each plot represent the range of Q for the respective watershed from WY's 1969–2012. Note the semi-log y axis on **(b)**.

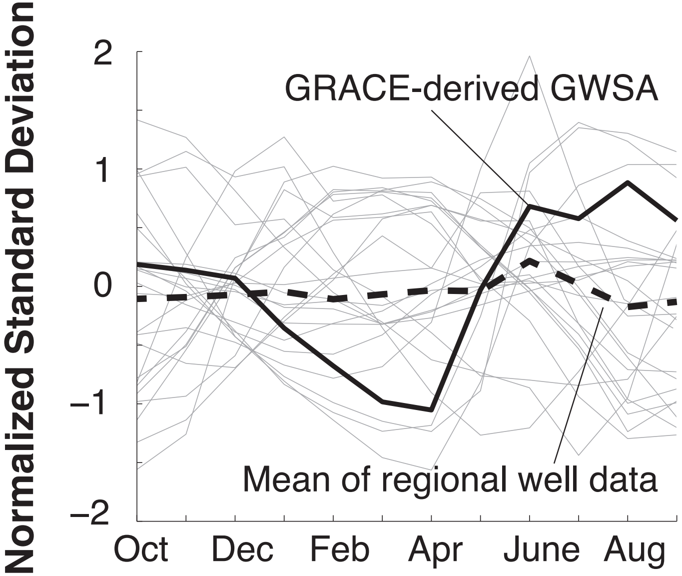

Figure 7. The normalized GRACE-derived groundwater anomaly compared to normalized well data over the study period. The grey lines in the background are the 33 individual wells, and the hashed line represents the mean of these wells. While some wells match the general GRACE-derived GWSA, variability across wells creates a muted mean signal.